ChemComm

Cite this: *Chem. Commun.*, 2011, **47**, 6093–6095

www.rsc.org/chemcomm

COMMUNICATION

Gold–platinum yolk–shell structure: a facile galvanic displacement synthesis and highly active electrocatalytic properties for methanol oxidation with super CO-tolerance†

Long Kuai, Shaozhen Wang and Baoyou Geng*

Received 7th December 2010, Accepted 7th April 2011
DOI: 10.1039/c0cc05429a

In this communication, we prepare a Au–Pt yolk–shell structure through a galvanic displacement strategy and explore its electrocatalytic properties for methanol oxidation. It exhibits high electrocatalytic activity with notable CO-tolerance.

In recent decades, numerous efforts have been made regarding the electrocatalytic oxidation of methanol for the great advantages and potential applications of direct methanol fuel cells (DMFCs).[1] Previous research suggests that platinum (Pt) is an excellent electrocatalyst for DMFCs.[2] But some crucial obstacles, including self-poisoning meaning a poor CO-tolerance,[3] low Pt utilization efficiency[4] and high-cost,[5] limit its development in commercial applications. Therefore, extensive research activities are being carried out to upgrade the performance of Pt catalysts.

Various strategies have been devoted to improving the performance of Pt catalysts. Generally, Pt catalysts are dispersed onto various supports to enhance their catalytic activity and increase the Pt utilization.[6] Moreover, several hollow Pt nanostructures exhibit an apparent modification of the catalytic activity observed for other Pt catalysts.[7] Very recently, porous Pt nanotubes and open-mouthed Pt microcapsules have been reported and these display much better catalytic activity than that of Pt/C or Pt powders.[8] Nevertheless, these hollow nanostructures, like other Pt nanostructures, also always suffer from poor CO-tolerance. Pt-based alloys, especially Pt/Ru, have been widely developed to enhance the CO-tolerance.[9] As expected, they certainly restrain the CO-poisoning effect to some extent. In addition, the cost of DMFCs with these catalysts is significantly lower. However, Pt-based alloy catalysts sometimes present lower activity and lower efficiency than pure Pt catalysts because their active surface is partly replaced by the less active component. Thus, it is still a challenge to design Pt-based catalysts with high CO-tolerance, low Pt-loading, high catalytic activity and long-term stability.

College of Chemistry and Materials Science, Anhui Key Laboratory of Functional Molecular Solids, Anhui Laboratory of Molecular-Based Materials, Anhui Normal university, Wuhu, 241000, P. R. China. E-mail: bygeng@mail.ahnu.edu.cn; Fax: (+86)-553-3869303

† Electronic supplementary information (ESI) available: Experimental section, UV-vis spectra, additional figures and figure captions. See DOI: 10.1039/c0cc05429a

Herein, we design a Pt-based catalyst with a unique structure for the electrocatalytic oxidation of methanol. This is a Au–Pt yolk–shell (Y–S) structure, obtained by a facile strategy by a galvanic displacement reaction, similar to that reported by Xia *et al.*[10] Typically, the Au@Ag core–shell (C–S) structure is fabricated by epitaxial growth of the Ag shell onto the Au core, and the Ag shell is subsequently displaced by H_2PtCl_6, so that the super thin hollow Pt shell forms naturally while the Au core are kept inside the hollow Pt shell. The mechanism is illustrated in Fig. 1a.

Similar structures (entitled nanorattles) have been paid some attention due to their unique optical properties and superior organic catalytic activity.[10,11] But the advantages for their electrocatalytic application in DMFCs are seriously

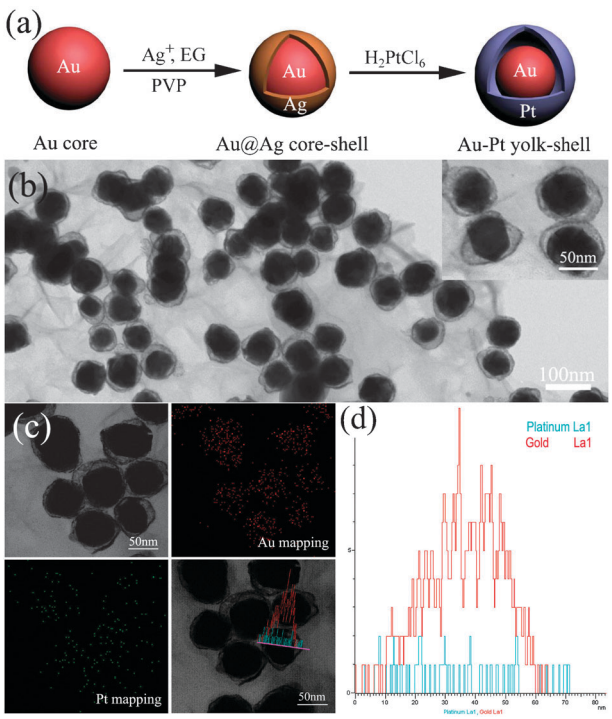

Fig. 1 (a) The formation mechanism of the Au–Pt Y–S structure; (b) a TEM image of the Au–Pt Y–S structure, the inset is a high-magnification image; (c) elemental mapping images; (d) cross-sectional compositional line profiles of the marked area in (c).

ignored. Here, we realize the unexplored advantages of the Au–Pt Y–S structure for the electrocatalytic oxidation of methanol. The Au–Pt Y–S structure is made up of a solid Au core and a hollow Pt shell, which is equal to the combination of a hollow Pt structure and a Pt-based alloy. So the problems of the Pt-based catalysts discussed above should, theoretically, be resolved. Firstly, the hollow Pt shell provides a high catalytic activity. Secondly, the Au–Pt Y–S structure is equivalent to the Pt-based alloy, which ensures the excellent CO-tolerance. To verify the theoretical speculation, we evaluated the electrocatalytic properties via electrocatalysis of the oxidation of methanol in alkaline media, for which reaction considerable achievements have been made[12] and less corrosion, more facile oxidation and less diffusion of methanol have been recognized using DMFCs.[13–15] As expected, a striking CO-tolerance and high catalytic activity were discovered. (1) The Au–Pt Y–S catalyst presents an amazing CO-tolerance with the I_f/I_b value reaching about 30 and over, while that of the other Pt-based catalysts is less than 10. (2) Unlike other Pt-based alloys, the higher CO-tolerance does not decrease the catalytic activity. It exhibits both the highest Pt-based mass and the highest specific activity among the catalysts mentioned below. (3) The overpotential decreases significantly compared to pure Pt catalysts, as it is negative-shifted by 47 mV and 52 mV compared to the hollow Pt and Pt NPs catalysts, respectively.

Fig. 1b is a typical TEM image of the Au–Pt Y–S structure and the inset is a high-magnification image, in which a solid core and a hollow shell can be observed. As can be seen, the Au–Pt Y–S structure is obtained as designed, with nearly 100% yield. Fig. 1c shows the elemental mapping investigation, revealing that the Au–Pt Y–S structure is made up of an Au core and a hollow Pt shell. The cross-sectional compositional line profiles (Fig. 1d and the lower right corner inset in Fig. 1c) further confirm the Au–Pt Y–S structure. In addition, the thickness of the Pt shell is 2–3 nm, which is equal to the diameter of about one or two Pt NPs.

The electrochemical properties of the Au–Pt Y–S catalyst were evaluated by using cyclic voltammetry. For comparison, the electrochemical measurements were also repeated with the Au@Pt core–shell (C–S, where there is no space between the Au core and Pt NPs, see Figs S7a and b†), hollow Pt (Figs S7c and d†), Pt NP, commercial Pt/C and Au NP catalysts under the same conditions. As displayed in Fig. 2a, typical hydrogen adsorption and desorption is observed. The electrochemically active surface areas (ESA) of the catalysts were obtained based on the hydrogen adsorption wave capacity (Q_H) with the following equation:[16]

$$A_{EL} = 0.1Q_H/(Q_{ref}\,(\text{Pt loading}))$$

where A_{EL} is expressed in $m^2\ g^{-1}$ Pt, Pt loading is given in mg cm^{-2} and $Q_{ref} = 0.21$ mC cm^{-2}, calculated from a surface density of 1.3×10^{15} atoms of Pt per cm^2. Consequently, the commercial Pt/C catalyst holds the highest ESA, which is consistent with previous reports.[8a,17] Moreover, the ESA for the Au–Pt Y–S catalyst is higher than the rest due to its unique structure. In addition, its ESA also exhibits good stability (see Fig. S8†).

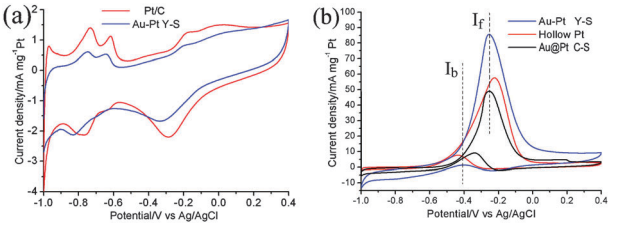

Fig. 2 (a) CVs of Au–Pt Y–S (blue line) and commercial Pt/C (red line) catalysts in 0.5 M N_2–saturated KOH aqueous solution, (b) CVs for a CH_3OH oxidation reaction catalyzed by Au–Pt Y–S (blue line), hollow Pt (red line) and Au@Pt C–S (black line) catalysts in 0.5 M KOH aqueous solution with 0.5 M CH_3OH in air.

The typical cyclic voltammograms (CVs) in Fig. 2b exhibit two obvious oxidation peaks. The current peak for the forward scan (I_f) is due to the oxidation of CH_3OH[18] and the removal of the carbonaceous intermediates is expressed by the current peak for the back scan (I_b).[19] Obviously, in the forward scan, the peak potential for CH_3OH oxidation on the Au–Pt Y–S catalyst is −0.254 V, which is negative-shifted by about 47 mV compared to that of the hollow Pt catalyst (−0.207 V) and nearly as the same as that of the Au@Pt C–S catalyst (−0.257 V). Moreover, compared with the Pt NP and commercial Pt/C catalysts (see Fig. S5†), the peak potential on the Au–Pt Y–S structure is even lower. So the overpotential in CH_3OH oxidation gets significantly reduced.

As shown in Table 1, the Au–Pt Y–S catalyst exhibits the highest specific activity (0.21 mA cm^{-2}, based on the ESA). In addition, although its mass activity is not apparent based on its metal content, the fact that it has the highest Pt-based mass activity is valuable for the research into low-Pt content catalysts. Therefore, the yolk–shell structure obviously enhances the electrocatalytic activity.

Previous reports have demonstrated that the anodic peak in the backward scan indicates the removal of CO-like carbonaceous species, which are not completely oxidized and accumulate on the catalyst surface during the forward scan.[18a] So the ratio of I_f/I_b can be used as an indicator of the CO-tolerance.[20] A lower ratio of I_f/I_b represents poorer oxidation of CH_3OH to the final product (CO_2) during the forward anodic scan and more accumulation of carbonaceous species on the surface of the catalyst. That is, a higher I_f/I_b value indicates a higher CO-tolerance. As displayed in Table 1, the Au–Pt Y–S catalyst has a much higher I_f/I_b value than the other four catalysts, confirming that CH_3OH molecules can be far more effectively oxidized to CO_2 during the forward anodic scan. Such a high I_f/I_b value indicates an unusual CO-tolerance. In addition, the CO-tolerance stability is also important. As shown in Fig. S9†, the Au–Pt Y–S catalyst exhibits excellent CO-tolerance stability. In addition, we found that a smaller Au core and larger space between the Au core and the Pt shell are beneficial to the electrocatalytic performance, as shown and discussed in Fig. S10†.

A series of experiments were undertaken to study the mechanism of the high CO-tolerance. To evaluate the role of the Au core, an electrochemical experiment was carried out with the hollow Pt catalyst, and the obtained I_f/I_b value was 9.1. Similarly, the electrochemical experiment was also repeated with the Au@Pt C–S catalyst to evaluate the role of

Table 1 Measurements taken from the electrooxidation of CH_3OH catalyzed by the various catalysts

Catalyst	ESA m^{-2} g^{-1} Pt	Peak potential/V	I_f/I_b	Mass activity/mA mg^{-1} Pt/Au–Pt	Specific activity/mA cm^{-2} Pt
Au–Pt Y–S	41.2	−0.254	29.9	86.1/21.5	0.21
Au–Pt C-R	29.9	−0.257	7.9	47.2/23.6	0.16
Hollow Pt	32.1	−0.207	9.1	57.4	0.18
Pt NPs/C	85.2	−0.252	6.7	41.1	0.05
Pt NPs	21.1	−0.205	4.8	23.6	0.11
Au NPs	0	—	—	—	—

the space between the Au core and the Pt shell, and the obtained I_f/I_b value was 7.9. Compared with the commercial Pt/C and Pt NPs catalysts, the alloy Au@Pt C–S and hollow Pt catalysts all have a higher I_f/I_b ratio. That is, Pt-based alloy and hollow Pt catalysts have the better CO-tolerance, which is in good agreement with previous reports.[7b,9a,c,21] Nevertheless, their improved CO-tolerance still looks rather bleak compared to the Au–Pt Y–S catalyst. Thus, maybe the collaborative effect of the Au core and the space between the Au core and the Pt shell play a key role in the high CO-tolerance. A possible explanation is proposed here. On the one hand, the bimetallic effect between the Pt and Au ensures that the as-prepared catalyst enhances the CO-tolerance. On the other hand, the space between the Pt shell and Au core makes the methanol molecule remain in the catalyst long enough for the methanol molecule to be oxidized efficiently. Therefore, the Au–Pt yolk–shell exhibits high CO-tolerance.

In summary, the Au–Pt yolk–shell structure is obtained and explored for electrocatalytic oxidation of methanol. The overpotential gets significantly reduced on Au–Pt yolk–shell catalyst. Notably, the high I_f/I_b value suggests that CH_3OH can be oxidized efficiently to CO_2 with much improved CO-tolerance. In addition, it exhibits the highest electrocatalytic activity. Thus, these advantages should make the Au–Pt yolk–shell catalyst available to be an attractive anodic catalyst for DMFCs.

This work was supported by the National Natural Science Foundation of China (20671003, 20971003), the Key Project of the Chinese Ministry of Education (209060), the Science and Technological Fund of Anhui Province for Outstanding Youth (10040606Y32) and the Program for Innovative Research Team at Anhui Normal University.

Notes and references

1 (*a*) C. Lamy, A. Lima, V. LeRhun, F. Delime, C. Coutanceau and J. M. Léger, *J. Power Sources*, 2002, **105**, 283; (*b*) M. W. Xu, G. Y. Gao, W. J. Zhou, K. F. Zhang and H. L. Li, *J. Power Sources*, 2008, **175**, 217; (*c*) V. D. Noto, E. Negro, R. Gliubizzi, S. Lavina, G. Pace, S. Gross and C. Maccato, *Adv. Funct. Mater.*, 2007, **17**, 3626.

2 (*a*) B. Lim, M. J. Jiang, P. H. C. Camargo, E. C. Cho, J. Tao, X. M. Lu, Y. M. Zhu and Y. N. Xia, *Science*, 2009, **324**, 1302; (*b*) L. Wang and Y. Yamauchi, *J. Am. Chem. Soc.*, 2010, **132**, 13636; (*c*) Z. M. Peng and H. Yang, *J. Am. Chem. Soc.*, 2009, **131**, 7542.

3 K. L. Nagashree and M. F. Ahmed, *Synth. Met.*, 2008, **158**, 610.

4 H. M. Zhang, W. Q. Zhou, Y. K. Du, P. Yang and C. Y. Wang, *Electrochem. Commun.*, 2010, **12**, 882.

5 S. J. Liao, K. A. Holmes, H. Tsaprailis and V. I. Birss, *J. Am. Chem. Soc.*, 2006, **128**, 3504.

6 (*a*) V. Mazumder and S. H. Sun, *J. Am. Chem. Soc.*, 2009, **131**, 4588; (*b*) Q. Wang, B. Y. Geng and B. Tao, *J. Power Sources*, 2011, **196**, 191; (*c*) X. Z. Cui, L. M. Guo, F. M. Cui, Q. J. He and J. L. Shi, *J. Phys. Chem. C*, 2009, **113**, 4134.

7 (*a*) Z. W. Chen, M. Waje, W. Z. Li and Y. S. Yan, *Angew. Chem., Int. Ed.*, 2007, **46**, 4060; (*b*) J. Zhao, W. X. Chen, Y. F. Zheng and X. Li, *J. Power Sources*, 2006, **162**, 168; (*c*) Z. M. Peng, J. B. Wu and H. Yang, *Chem. Mater.*, 2010, **22**, 1098; (*d*) S. J. Guo, S. J. Dong and E. K. Wang, *Chem.–Eur. J.*, 2008, **14**, 4689.

8 (*a*) S. M. Alia, G. Zhang, D. Kisailus, D. S. Li, S. Gu, K. Jensen and Y. S. Yan, *Adv. Funct. Mater.*, 2010, **20**, 3742; (*b*) S. Mandal, M. Sathish, G. Saravanan, K. K. R. Datta, Q. M. Ji, J. P. Hill, H. Abe, I. Honma and K. Ariga, *J. Am. Chem. Soc.*, 2010, **132**, 14415.

9 (*a*) S. J. Guo, S. J. Dong and E. K. Wang, *ACS Nano*, 2010, **4**, 547; (*b*) Z. F. Liu, J. E. Hu, Q. Wang, K. Gaskell, A. I. Frenkel, G. S. Jackson and B. Eichhorn, *J. Am. Chem. Soc.*, 2009, **131**, 6924; (*c*) S. Zhang, Y. Y. Shao, G. P. Yin and Y. H. Lin, *Angew. Chem., Int. Ed.*, 2010, **49**, 2211; (*d*) J. C. Huang, Z. L. Liu, C. B. He and L. M. Gan, *J. Phys. Chem. B*, 2005, **109**, 16644.

10 Y. G. Sun, B. Wiley, Z. Y. Li and Y. N. Xia, *J. Am. Chem. Soc.*, 2004, **126**, 9399.

11 (*a*) Y. Khalavka, J. Becker and C. Sönnichsen, *J. Am. Chem. Soc.*, 2009, **131**, 1871; (*b*) J. H. Yang, L. H. Lu, H. S. Wang and H. J. Zhang, *Scr. Mater.*, 2006, **54**, 159; (*c*) K. Kamata, Y. Lu and Y. N. Xia, *J. Am. Chem. Soc.*, 2003, **125**, 2384; (*d*) J. H. Gao, G. L. Liang, B. Zhang, Y. Kuang, X. X. Zhang and B. Xu, *J. Am. Chem. Soc.*, 2007, **129**, 1428.

12 (*a*) F. Ksar, G. Surendran, L. Ramos, B. Keita, L. Nadjo, E. Prouzet, P. Beaunier, A. Hagège, F. Audonnet and H. Remita, *Chem. Mater.*, 2009, **21**, 1612; (*b*) J. P. Liu, J. Q. Ye, C. W. Xu, S. P. Jiang and Y. X. Tong, *J. Power Sources*, 2008, **177**, 67; (*c*) P. V. Samant, J. B. Fernandes, C. M. Rangel and J. L. Figueiredo, *Catal. Today*, 2005, **102–103**, 173; (*d*) X. Z. Fu, Y. Liang, S. P. Chen, J. D. Lin and D. W. Liao, *Catal. Commun.*, 2009, **10**, 1893.

13 (*a*) F. Bidault, D. J. L. Brett, P. H. Middleton and N. P. Brandon, *J. Power Sources*, 2009, **187**, 39; (*b*) J. S. Guo, A. Hsu, D. Chu and R. R. Chen, *J. Phys. Chem. C*, 2010, **114**, 4324.

14 J. S. Spendelow and A. Wieckowski, *Phys. Chem. Chem. Phys.*, 2007, **9**, 2654.

15 Y. Xiong, Q. L. Liu, A. M. Zhu, S. M. Huang and Q. H. Zeng, *J. Power Sources*, 2009, **186**, 328.

16 D. Villers, S. H. Sun, A. M. Serventi and J. P. Dodelet, *J. Phys. Chem. B*, 2006, **110**, 25916.

17 S. H. Sun, G. X. Zhang, D. S. Geng, Y. G. Chen, M. N. Banis, R. Y. Li, M. Cai and X. L. Sun, *Chem.–Eur. J.*, 2010, **16**, 829.

18 (*a*) M. M. Dimos and G. J. Blanchard, *J. Phys. Chem. C*, 2010, **114**, 6019; (*b*) J. B. Jia, L. Y. Cao and Z. H. Wang, *Langmuir*, 2008, **24**, 5932.

19 (*a*) A. Halder, S. Sharma, M. S. Hegde and N. Ravishankar, *J. Phys. Chem. C*, 2009, **113**, 1466l; (*b*) Y. J. Gu and W. T. Wong, *Langmuir*, 2006, **22**, 11447.

20 R. Manohara and J. B. Goodenough, *J. Mater. Chem.*, 1992, **2**, 875.

21 H. Ren, M. P. Humbert, C. A. Menning, J. G. Chen, Y. Y. Shu, U. G. Singh and W. C. Cheng, *Appl. Catal., A*, 2010, **375**, 303.